Received: 4 June 2023, Accepted: 24 July 2023, Published: 29 December 2023 Publisher: UTP Press, Creative Commons: CC BY 4.0

AG_2O NANOPARTICLE AND ITS COMPOSITE WITH COORDINATION POLYMERS OF CU: SYNTHESIS, CHARACTERISATION AND PHOTOCATALYTIC ACTIVITY

Reazul Hasan Riyan[1], Md. Azharul Arafath[1*], Syed Shamsul Alam[1] and Muhammad Omar Faruk[2]

[1]Department of Chemistry, Shahjalal University of Science and Technology, Bangladesh
[2]Department of Physics, Shahjalal University of Science and Technology, Bangladesh

*E-mail: arafath-che@sust.edu

ABSTRACT

In this study, we report the synthesis, characterisation, and photocatalytic activity evaluation of Ag_2O nanoparticles (NPs) and their composite, Ag_2O/Cu-CP, with coordination polymers (CPs) of Cu. Ag_2O NPs were synthesised using the coprecipitation method. The composite was prepared via the sonication method. FTIR and XRD patterns revealed the formation of the nanoparticles and composite. Photocatalytic activity of the NPs and Composite was performed under solar irradiation for Methylene Blue (MB) as a dye. The photocatalytic degradation efficiency was monitored for concentration decay over time using UV-Vis. Spectrophotometer. The synthesised Ag_2O/Cu-Cp composite showed a degradation efficiency of 97.59%, whereas Ag_2O NPs showed an efficiency of 82.23%. The composite exhibited 1.18 times higher activity than Ag_2O NPs. The band gap plays a crucial role in enhancing activity. The incorporation of Cu-Cp with Ag_2O NPs reduced the band gap to an optimum level for radical formation. So, this kind of composite could be widely used in the effluent treatment of industry for a green environment.

Keywords: *Ag_2O nanoparticles, composite, powder-XRD, dye degradation, photocatalytic activity, UV-vis spectroscopy.*

INTRODUCTION

Nanoscience is very important for every sector of science and technology. Researchers were exploring more features of nano-sized materials, which include metal oxide nanoparticles, carbon nanotubes, metal-organic frameworks, nano-natural polymers, etc. Nano-sized materials can be organic or inorganic in nature and have distinctive characteristics owing to their very small size and increased surface area compared to larger particles of the same material. Nanoparticles are appealing for a wide variety of applications, including catalysis, sensing, and environmental remediation [1]. In recent years, the field of nanoscience has witnessed significant advancements, leading to the establishment of various functional materials possessing distinctive characteristics and potential applications. Among these, Ag_2O nanoparticles have gained significant attention due to their remarkable photocatalytic activity and suitable applications in diverse fields [2].

Metal oxide nanoparticles have the potential to operate as a visible, photocatalytic catalyst for deterioration caused by a narrowing bandgap. Due to their exceedingly high selectivity and photocatalytic activity, Ag_2O NPs have recently become one of the most widely used photocatalysts. The photocatalytic activity of Ag-containing catalysts, such as Ag_2CO_3, Ag_3VO_4, Ag_3PO_4, and Ag_2O, for the degradation of persistent organic pollutants is exceptional [3]. This contrasts with other photocatalysts driven by visible light, such as $BiVO_3$, N-TiO_2, and ZnS. The method of photocatalysis has advanced significantly because of this innovation. Examples of applications for silver oxide nanoparticles with a cubic structure and a lattice parameter of 0.472 nm include cleaning agents, electrode materials, catalysts, preservatives, and colourants for the activation of alkanes and olefins [2].

Nanocomposites showed extensive behaviour compared to their parent nanoparticles. Ullah et al. [4] synthesised silver-morphine-functionalised polypropylene (AgPP-mrp) nanocomposite and performed dye degradation against methyl orange. The AgPP-mrp catalyst demonstrated more effective degradation capabilities within a short timeframe when placed under solar irradiation. Zhang et al. [5] Ag_2O/g-C_3N_4/Fe_3O_4 nanocomposites fabricated by coprecipitation method. It has been determined that this phenomenon can be accounted for by the fact that the presence of extra photocatalysts results in a discernible decrease in the amount of light transmission. As a result, nanocomposites composed of Ag_2O/g-C_3N_4/Fe_3O_4 were utilised in the subsequent photocatalysis. Laouini et al. [6] synthesised Ag/Ag_2O nanoparticles utilising green methods and performed dye degradation against methylene blue (MB) dye.

Coordination polymers (CP) and metal-organic frameworks (MOFs) have achieved considerable focus in the last few years due to their exclusive characteristics and potential applications in numerous fields. Coordination polymers have tunable pore size, high surface area and are easily synthesised from a vast number of metal ions and organic ligands, making them an attractive material for gas storage, separation, and catalysis [7]. Functional characteristics of the CP include the capacity to separate gas, store gases and liquid mixtures, electrochemical, catalytic, and water purification, biomedical applications, attractive applications in fluorescence sensing, absorption, molecular magnetism, and heterogeneous catalysis [8]-[18].

Metal-organic frameworks (MOFs) are efficient photocatalysts in sunlight to remove methylene blue in an aqueous medium. MOFs retain their stability even after five cycles of catalytic activity. Hydroxyl radicals and holes are the species involved in the mechanism of dye degradation [19]. Saemian et al. [20] fabricated a composite of Cu MOF named after $CoFe_2O_4$/SiO_2/Cu-MOF and performed dye degradation against methylene blue. According to their findings, almost all the MB solutions present in the model effluent sample were degraded after 1 hour. Abdollahi et al. [21] utilised solar light to observe the catalysis property of Cu-MOF in dye degradation reactions. Ag_2CrO_4/Cu (BDC) MOFs photocatalysts with various mass percentages of Cu (BDC) were fabricated for water refining applications in the presence of sunlight. Furthermore, the existence of Cu (BDC) increased light absorption and reduced the rate of recombination of electron-hole pairs. Jin et al. [22] synthesised Cu-CP and observed the photocatalytic properties of the fabricated material. Cu(II)-based CP $[Cu_2(HL)_2(bib)_2]$ exhibits enhanced photocatalytic activity for the degradation of MB and is also recyclable. Zhai et al. [23] fabricated unsaturated copper (II) CP, $[Cu(tptc)_{0.5}(bpy)(H_2O)]_n$ dye degradation was performed in the presence of this synthesised material. This material demonstrates an outstanding degree of efficacy in the process of photocatalytic degradation of MB under UV irradiation.

Ag_2O NPs possess excellent catalytic properties, high surface area, and unique electronic and optical properties [24]. They are known to exhibit strong visible light absorption and efficient charge carrier separation, making them promising candidates for photocatalytic applications. Incorporating Ag_2O NPs into coordination polymers of Cu form composite can synergistically combine the advantages of both materials, leading to enhanced photocatalytic activity.

EXPERIMENTAL

Materials and Methods

Material

The chemicals $AgNO_3$ (99%) and NaOH (≥ 97%) were purchased from Sigma Aldrich. Methylene Blue (MB) (82%), which was used as a model pollutant, was bought from PT. Smart Lab Indonesia. The reagents utilised in the experiment were of analytical grade and did not require any additional purification.

Methods

The Fourier-transform infrared (FT-IR) spectra were acquired using an IR Prestige-21, Shimadzu Corporation, Japan instrument on KBr disks, covering a wavenumber range of 4,000 to 400 cm^{-1}. The UV–Vis spectra were recorded on a UV–Vis Spectrophotometer (UV-1800 Series Shimadzu spectrometer) in DI water solvent and spectra were collected using this spectrophotometer under a wavelength range of 200 to 800 nm. Powder-XRD analysis was carried out with a Smart-Lab X-ray Diffractometer by Rigaku Corporation. The diffraction patterns were captured in 1D step scan mode with 0.010 m step width. The X-ray generator's parameters were 40 kV and 75 mA, while the filter was a K_β filter for copper, the selector slit was BB, and the detector was a D/teX Ultra 25°C. The diffraction patterns were obtained between 15° and 80° for two angles. The scanning speed was 20.00°/min.

Synthesis of Compounds

Synthesis of Ag_2O Nanoparticles

A 100 mL of 0.015 M silver nitrate aqueous solution was prepared in the beaker and heated to 70°C. Then, 20 mL of 0.095 M sodium hydroxide aqueous solution was added dropwise with continuous stirring (Figure 1). The resultant solution was stirred and heated at 70°C until the solution turned to a greyish colloidal suspension. The product was repeatedly washed and centrifuged with water, and the brown Ag_2O nanoparticles were recovered. Then, the product was dried under a vacuum and kept in a desiccator.

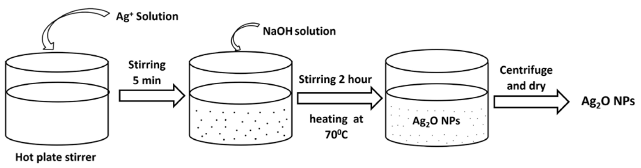

Figure 1 The flow chart shows the synthesis of Ag_2O NPs

Synthesis of Ag_2O/Cu-CP Composite

A 25 mL of 25% Ag_2O colloidal suspension was prepared in a 100 mL beaker. Then, 25 mL of 75% Cu-CP colloidal suspension was added to the Ag_2O suspension. The resultant suspension was sonicated for 30 minutes (Figure 2).

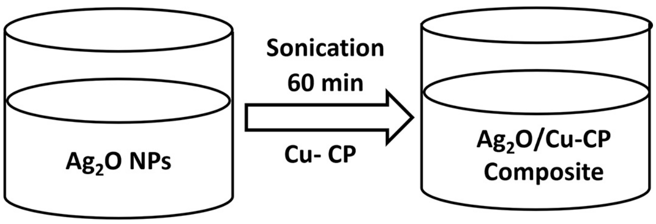

Figure 2 The synthesis of Ag_2O/Cu-CP composite by the reaction between Ag_2O and Cu-CP by sonication

The product was repeatedly washed and centrifuged with water, and the greenish-black Ag_2O/Cu-CP composite was recovered. Then, the product was dried under a vacuum pump and kept in a desiccator.

Photocatalytic Activity

The photocatalytic activities of Ag_2O NPs and Ag_2O/Cu-CP composite were investigated under sunlight irradiation. A series of MB diluted solutions was prepared from 5 ppm to 10 ppm. The quantity of catalyst was 0.05% throughout the investigation, and pH was maintained at 9.2. Then, the solution was kept in the dark for 30 minutes. After that, the solution was collected, and absorbance was measured by UV-Vis spectroscopy. Then, the solution was irradiated by sunlight with continuous stirring, and the sample was collected to measure absorbance at 15/20 minutes intervals. The data was collected over 60 minutes. The percentage of dye degradation was calculated using the following equation [25].

$$\text{Degradation Efficiency (\%)} = \frac{(C_o\text{-}C_t)}{(C_o)} \times 100 \quad (1)$$

where, C_o = Initial Concentration of MB
and C_t = Concentration at (t) time

RESULT AND DISCUSSION

FTIR Spectroscopy

The chemical structure of Cu-CP, Ag_2O NPs, and Cu-CP/Ag_2O composite is studied by FTIR spectroscopy. The dispersion of Ag_2O nanoparticles in the polymer matrix has been confirmed through FTIR spectrum analysis. The vibrations of Ag-O and O-Ag-O are assigned to the peaks at 883.89 and 696.40 cm^{-1}, respectively. Additionally, the band at 489 cm^{-1} appears by combining two bands attributed to the stretch and bend modes of Ag-O and Ag-O-Ag.

In the IR spectra of Cu-CP (Figure 3), the υ(O-H) stretch vibrations and the υ(N-H) stretch vibrations were observed at 3591.45 cm^{-1} to 3286.70 cm^{-1}. Stretches in 3151.68 cm^{-1}, 1373.31 cm^{-1}, 1473.61 cm^{-1}, 1408.03 cm^{-1} indicate that there is a benzene ring in the Cu-CP. Broad frequency in the 1649 cm^{-1} region indicates the C=O functional group, and the peaks belonging to the υ(C=N) and υ(C=C) stretch vibrations appear from 1647.20 cm^{-1} and 1612.49 cm^{-1}. Other peaks in the fingerprint region, such as 483 cm^{-1}, could indicate Cu-O or Cu-N bonding. The υ(C-H) stretch vibrations of the 4,4′-Trimethylenedipyridine ligand were observed at 1106.84 cm^{-1} and 837.10 cm^{-1}.

In the IR spectra of the Ag_2O/Cu-CP composite (Figure 3), the peaks at 889.322 cm^{-1} and 687.74 cm^{-1} are allotted to vibrations of Ag–O and O–Ag–O. The υ(O-H) stretch vibrations were observed at 3656.94 cm^{-1} to 3052.47 cm^{-1}. It became a broader peak due to composite formation as the bond in composite formation is assumed with polar atoms such as oxygen or nitrogen. The υ(N-H) stretch vibrations were observed at 2326.32 cm^{-1} and 2356.94 cm^{-1}. Stretches in 1392.14 cm^{-1} indicate that there is a benzene ring in the Cu-CP. Broad frequency in the 1659.05 cm^{-1} region indicates the C=O functional group. The υ(C-H) stretch vibrations belonging to the 4,4′-Trimethylenedipyridine ligand were observed at 1122.88 cm^{-1}. The displacement of peaks has proven the composite formations.

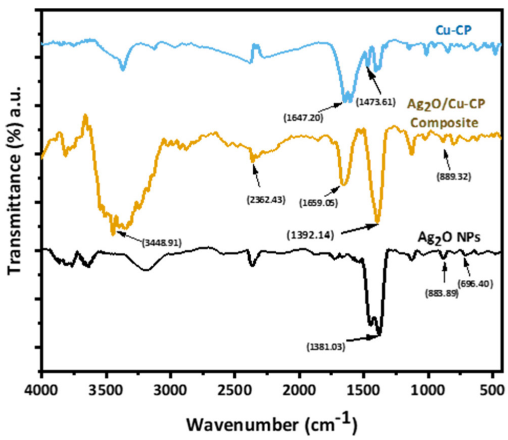

Figure 3 FTIR spectra of (a) Cu-Cp, (b) Cu-CP/Ag_2O composite and (c) Ag_2O NPs

X-Ray Diffraction Analysis

An X-ray diffraction (XRD) pattern of the produced sample was acquired to determine the phase composition of the metal oxide. Using Scherer's formula, the particle size was calculated as:

$$D = K\lambda / \beta \cos\theta \quad (2)$$

where, K is 0.94, λ is the wavelength of $Cu\text{-}K_\beta$ radiation X-ray (λ = 1.39 Å), and β is the full width at half maximum (FWHM) of the diffraction peak, which corresponds to 2θ and θ is Bragg's angle. The wavelength of utilised X-ray, which is Cu-K_β radiation (λ = 1.39 Å), θ is the peak position in radians, n is the order of diffraction, which was 1, and d is represented as interplanar spacing in Å [26]-[27].

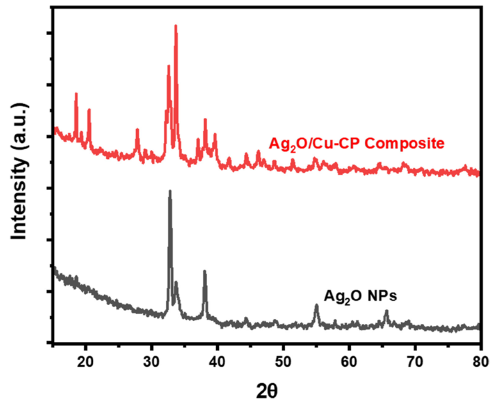

Figure 4 X-ray diffraction of Ag_2O NPs and Ag_2O/Cu-CP Composite

The Ag_2O nanoparticles were analysed using X-ray diffraction (XRD) analysis to evaluate the level of crystallisation and the purity of the anticipated phases, i.e., size and composition (Figure 4). The XRD spectrum indicates the crystalline form of the particles. The diffraction angles of 32.7795°, 34.12791°, and 38.05644° (PDF file number 77-1829) correspond to the diffraction peak observed in the X-ray diffraction pattern of crystalline Ag_2O. So, the XRD pattern can provide enough evidence to confirm the successful formation of Ag_2O NPs, which have high purity. The average crystal size was calculated using Debye Scherer's formula. The average crystal size was found to be 50.06958 nm (Table 1).

Table 1 A table of peak position (2θ) of XRD data of Ag_2O

Peak position (2θ)	θ (°)	FWHM	Crystal Size D (nm)	Average D (nm)
32.7795	16.38975	0.32057	25.831	
34.12791	17.06396	0.08535	97.365	50.069
38.05644	19.02822	0.3111	27.012	

XRD analysis was carried out on the Ag_2O/Cu-CP Composite. The XRD spectrum shows that the particles are crystalline. A significant change appears in the peak position of the Ag_2O/Cu-CP composite from Ag_2O. The diffraction peak for crystalline Ag_2O/Cu-CP composite appears at 2θ diffraction angle at 18.52774°, 20.43415°, 33.6577° and 38.11226°. The displacement of the peak position prefers the formation of the composite. The average crystal size was found to be 17.8658nm (Table 2).

Table 2 A table of peak position (2*θ*) of XRD data of Ag_2O/Cu-CP composite

Peak position (2*θ*)	*θ* (°)	FWHM	Crystal Size D (nm)	Average D (nm)
18.52774	9.26387	0.44913	17.922	
20.43415	10.21708	0.44989	17.943	17.8658
33.65771	16.82886	0.49688	16.704	
38.11226	19.05613	0.44482	18.895	

Photodegradation of Dyes Using Ag_2O Nps and Ag_2O/Cu-CP Composite

The investigation of photocatalytic activity in the degradation of Methylene Blue in wastewater significantly depends on time. The dye concentration decreased consistently over time (0 to 60 minutes), as shown in Figure 5. The peaks from the UV-vis spectrometer are taken to observe the degradation capacity of Ag_2O NPs and Ag_2O/Cu-CP composite (Figure 5).

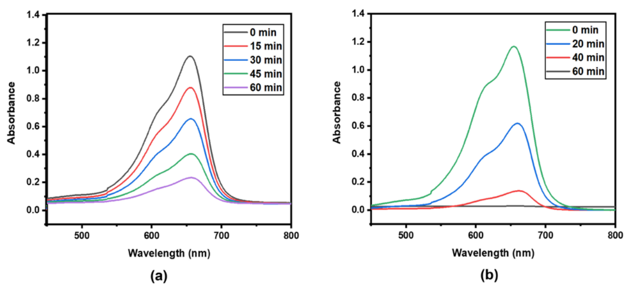

Figure 5 The degradation of MB by (a) Ag_2O NPs (b) Ag_2O/Cu-CP composite

The captivating phenomenon was observed in Figure 5b, where the absorption peak of MB dye was decreased sharply under sun irradiation in the case of Ag_2O/Cu-CP composite than Ag_2O NPs, which were used as photocatalysts. When all the measurements are made using the same cuvette, the Beer-Lambert equation states that the Concentration is directly proportional to the absorption. As the absorbance was found to be decreasing, the Concentration of MB fell as a direct result of these findings. It is the primary proof that catalysis was involved in the degradation of the dye. When subjected to UV light irradiation, the electron of oxygen (O) in the Ag_2O/Cu-CP system can undergo a transition from the highest occupied orbital (HOMO) to the lowest unoccupied orbital (LUMO) of the central ion. To achieve stability, the highest occupied molecular orbital (HOMO) necessitated the capture of an electron from a water molecule, resulting in the formation of a hydroxyl radical ($^{\cdot}OH$). These radicals exhibit potent oxidation capabilities selectivity to methylene blue (MB) molecules that contain abundant nitrogen atoms [28]. The CP can trap light until significant time for photocatalytic activities due to the porosity of the molecules.

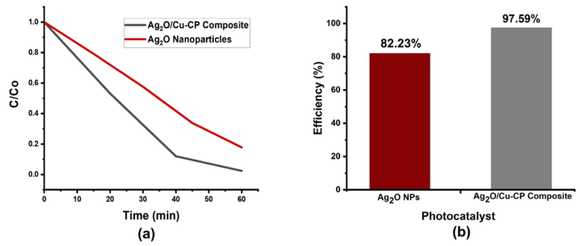

Figure 6 (a) The decreasing manner of C/C_o and (b) efficiency after 60 min of MB degradation by Ag_2O NPs, Ag_2O/Cu-CP composite photocatalyst

Table 3 Observing degradation efficiency of synthesised materials

Materials	Time (min)	Abs	A/Ao = C/C_o	Degradation efficiency = $(1-C/C_o)$* 100%
	0	0.698(Ao)	1	0
Ag_2O NPs	15	0.553	0.792	20.77363897
	30	0.402	0.576	42.40687679
	45	0.236	0.338	66.18911175
	60	0.124	0.178	82.23495702
Ag_2O/Cu-CP Composite	0	1.163(Ao)	1	0
	20	0.619	0.532	46.7755804
	40	0.139	0.12	88.04815133
	60	0.028	0.024	97.59243336

The value of the ratio of concentration and beginning concentration (C/C_o) decreased over time in the presence of Ag_2O NPs and Ag_2O/Cu-CP composite.

The C/C_0 data was therefore made sure to follow a decreasing pattern (Figure 6a). Consequently, the degradation catalysis was clearly visible with effective efficiency (Table 3). After 60 minutes, the degradation efficiency was 82.23% in the presence of an Ag_2O NPs catalyst and 97.59% in the presence of an Ag_2O/Cu-CP composite catalyst (Figure 6b).

CONCLUSION

In summary, Ag_2O and Ag_2O/Cu-CP composite have been prepared by coprecipitation and sonication methods. The XRD pattern and FTIR spectroscopic analysis revealed the formation of Ag_2O NPs and Ag_2O/Cu-CP composite. The particles exhibit an average crystallite size within the range of 50-55 nm for Ag_2O NPs and 17-20 nm for composite. Furthermore, Cu-CP can potentially expedite the separation of charges and decrease the band gap. Ag_2O/Cu-CP composite exhibits extensive photocatalytic activity on the degradation of MB with respect to Ag_2O NPs under solar irradiation. Therefore, the Ag_2O/Cu-CP composite is a suitable contender in wastewater treatment to remove contaminants.

ACKNOWLEDGMENT

The authors wish to thank Shahjalal University of Science and Technology, Research Center for the Promotional Research Grant (Project ID: PS/2022/1/07, 2022-2023).

Conflict of interest: There is a conflict of interest to declare.

REFERENCES

[1] G. Oskam, "Metal oxide nanoparticles: synthesis, characterisation and application," *Journal of Sol-Gel Science and Technology*, vol. 37, pp. 161-164, 2006.

[2] W. M. Shume, H. C. A. Murthy, and E. A. Zereffa, "A review on synthesis and characterisation of Ag_2O nanoparticles for photocatalytic applications," *Journal of Chemistry*, vol. 2020, pp. 1-15, 2020.

[3] A. Habibi-Yangjeh and B. Golzad-Nonakaran, "Fabrication of magnetically recoverable nanocomposites by combination of Fe_3O_4/ZnO with AgI and Ag_2CO_3, Substantiallyenhanced photocatalytic activity under visible light," *Physical Chemistry Research*, vol. 6, no. 2, pp. 415-431, 2018.

[4] R. Ullah, M. Tuzen, and B. Hazer, "Novel silver-morphine-functionalised polypropylene (AgPP-mrp) nanocomposite for the degradation of dye removal by multivariate optimisation approach," *Environmental Science and Pollution Research*, vol. 30, pp. 79904-79915, 2023.

[5] D. Zhang, S. Cui, and J. Yang, "Preparation of Ag_2O/g-C_3N_4/Fe_3O_4 composites and the application in the photocatalytic degradation of Rhodamine B under visible light," *Journal of Alloys and Compounds*, vol. 708, pp. 1141-1149, 2017.

[6] S. E. Laouini, A. Bouafia, A. V. Soldatov, H. Algarni, M. L. Tedjani, G. A. M. Ali, and A. Barhoum, "Green synthesised of Ag/Ag_2O nanoparticles using aqueous leaves extracts of Phoenix dactylifera L. and their azo dye photodegradation," *Membranes*, vol. 11, no. 7, p. 468, 2021.

[7] S. T. Meek, J. A. Greathouse, and M. D. Allendorf, "Metal-organic frameworks: A rapidly growing class of versatile nanoporous materials," *Advanced Materials*, vol. 23, no. 2, pp. 249-267, 2010.

[8] R.-B. Lin, S. Xiang, W. Zhou, and B. Chen, "Microporous Metal-Organic Framework Materials for Gas Separation," *Chem*, vol. 6, no. 2, pp. 337–363, 2020.

[9] A. Y. Tsivadze, O. E. Aksyutin, A. G. Ishkov, …E. V. Khozina, and V. A. Grachev, "Metal-organic framework structures: Adsorbents for natural gas storage," *Russian Chemical Reviews*, vol. 88, no. 9, pp. 925–978, 2019.

[10] J. -R. Li, J. Sculley, and H. -C. Zhou, "Metal-organic frameworks for separations," *Chemical Review*, vol. 112, pp. 869–932, 2012.

[11] H. Cai, Y. -L. Huang, and D. Li, "Biologicalmetal–organic frameworks: Structures, host–guest chemistry and bio-applications," *Coordination Chemistry Reviews*, vol. 378, pp. 207–221, 2019.

[12] A. Dhakshinamoorthy, A. M. Asiri, and H. García, "Metal–Organic Frameworks as Multifunctional Solid Catalysts," *Trends in Chemistry*, vol. 2, no. 5. pp. 454–466, 2020.

[13] Y.-S. Kang, Y. Lu, K. Chen, Y. Zhao, P. Wang, and W.-Y. Sun, "Metal–organic frameworks with catalytic centres: From synthesis to catalytic application," *Coordination Chemistry Reviews*, vol. 378, pp. 262–280, 2019.

[14] Y. Cui, Y. Yue, G. Qian, and B. Chen, "Luminescent functional metal-organic frameworks," *Chemical Reviews*, vol. 112, no. 2, pp. 1126– 1162, 2012.

[15] J. Yu, L. -H. Xie, J. -R. Li, Y. Ma, J. M. Seminario, and P. B. Balbuena, "CO_2 Capture and Separations Using MOFs: Computational and Experimental Studies," *Chemical Reviews*, vol. 117, no. 14, pp. 9674–9754, 2017.

[16] D. N. Woodruff, R. E. P. Winpenny, and R. A. Layfield, "Lanthanide Single-Molecule Magnets," *Chemical Reviews*, vol. 113, no. 7, pp. 5110–5148, 2013.

[17] H. Zhang, G. Liu, L. Shi, H. Liu, T. Wang, and J. Ye, "Engineering coordination polymers for photocatalysis," *Nano Energy*, vol. 22, pp. 149–168, 2016.

[18] J. Yang, P. Xiong, C. Zheng, H. Qiu, and M. Wei, "Metal–Organic Frameworks: A New Promising Class of Materials for a High-Performance Supercapacitor Electrode," *Journal of Materials Chemistry A*, vol. 2, no. 39, pp. 16640–16644, 2014.

[19] S. T. Karunakaran, R. Pavithran, M. Sajeev, and S. M. M. Rema, "Photocatalytic degradation of methylene blue using a manganese-based metal organic framework," *Results in Chemistry*, vol. 4, p. 100504, 2022.

[20] T. Saemian, M. H. Sadr, M. T. Yaraki, M. Gharagozlou, and B. Soltani, "Synthesis and characterisation of $CoFe_2O_4$/SiO_2/Cu-MOF for degradation of methylene blue through catalytic sono-Fenton-like reaction," *Inorganic Chemistry Communications*, vol. 138, p. 109305, 2022.

[21] B. Abdollahi, S. Farshnama, E. A. Asl, A. Najafidoust, and M. Sarani, "Cu (BDC) metal–organic framework (MOF)-based Ag_2CrO_4 heterostructure with enhanced solar-light degradation of organic dyes," *Inorganic Chemistry Communications*, vol. 138, p. 109236, 2022.

[22] J. Jin, K. Wang, M. Afzal, …L. Botha and W. Chang, "New Cu (II)-based three-dimensional supramolecular coordination polymer as photocatalyst for the degradation of methylene blue," *Journal of Molecular Structure*, vol. 1266, p. 133533, 2022.

[23] L. Zhai, Y. Niu, X. Chen, …B. Li and L. Fan, "Crystal structure, electrochemical reversibility, and photocatalytic degradation of a coordination unsaturated copper (II) based coordination polymer," *Inorganic Chemistry Communications*, vol. 119, p. 108121, 2020.

[24] L. Feng, G. Gao, P. Huang, K. Wang, X. Wang, T. Luo, and C. Zhang, "Optical properties and catalytic activity of bimetallic gold-silver nanoparticles," *Nano Biomedicine and Engineering*, vol. 2, no. 4, pp. 258-267, 2010.

[25] X. Zhang, G. Zhou, H. Zhang, C. Wu, and H. Song, "Characterisation and activity of visible light–driven TiO_2 photocatalysts co-doped with nitrogen and lanthanum," *Transition Metal Chemistry*, vol. 36, pp. 217–222, 2011.

[26] A. H. Moharram, S. A. Mansour, M. A. Hussein, and M. Rashad, "Direct precipitation and characterisation of ZnO nanoparticles," *Journal of Nanomaterials*, vol. 2014, pp. 20-20, 2014.

[27] M. A. Ismail, K. K. Taha, A. Modwi, and L. Khezami, "ZnO nanoparticles: Surface and X-ray profile analysis," *Journal of Ovonic Research*, vol. 14, no. 5, pp. 381-393, 2018.

[28] L. Lu, J. Wang, C. Shi, Y. Sun, W. Wu, Y. Pan, and M. Muddassir, "Four structural diversity MOF-photocatalysts readily prepared for the degradation of the methyl violet dye under UV-visible light," *New Journal of Chemistry*, vol. 45, no.2, pp. 551-560, 2021.